Supporting Information.

An Energy-Efficient Tellurium Electrode Enabled by Cs_2TeI_6 Perovskite Structure for Durable Aqueous Zn–Te Batteries

Jinye Li, Chengjun Lei, Pengjie Jiang, Chen Xu, Tingting Liu, Xiao Liang*

State Key Laboratory of Chem/Bio-Sensing and Chemometrics, Joint International Research Laboratory of Energy Electrochemistry, College of Chemistry and Chemical Engineering, Hunan University, Chang-sha 410082, China

* Corresponding author: xliang@hnu.edu.cn

Materials

All reagents were used as received without any further purification. Anhydrous zinc sulfate ($ZnSO_4$), lithium chloride (LiCl), potassium chloride (KCl), cesium chloride (CsCl), lithium bromide (LiBr), potassium bromide (KBr), cesium bromide (CsBr), lithium iodide (LiI), potassium iodide (KI), cesium iodide (CsI), acetic acid, hydrochloric acid (HCl), hydrobromic acid (HBr), hydroiodic acid (HI), tellurium dioxide (TeO_2) were purchased from Sigma-Aldrich.

Preparation of Te cathodes

Elemental Tellurium (Te, 99.99 %, Sigma-Aldrich) and Ketjen Black (KB) were mixed at a weight ratio of 60:40 by mechanically ball milling for 4 hours, and then the KB/Te was transferred to a vacuum quartz tube and heated at 480 °C for 24 h. The Te electrode were prepared by mixing 80 wt% KB/Te, 10 wt% Super-P carbon and 10 wt% PVDF binder in NMP solvent, followed by doctor-blading the slurry on Ti mesh. The electrode was vocuum dried at 60 °C for 24 h. The typical Te areal loading on each electrode was about 1.5 mg cm^{-2}. The electrode composition was precisely controlled during the lean electrolyte evaluation (10 μL), in which CsI was blended with Te to prepare the electrode. The molar ratio of iodine ions to Te in the cell has to reach 6:1 to accomplish the Cs_2TeI_6 formation.

Synthesis of A_2TeX_6

The A_2TeX_6(X=Cl, Br, I) could be prepared by follow approaches:

$$TeO_2 + 4HCl \rightarrow TeCl_4 + 2H_2O \quad \text{(S1)}$$

$TeCl_4 + 2CsCl \rightarrow Cs_2TeCl_6$ (S2)

$TeO_2 + 4HBr \rightarrow TeBr_4 + 2H_2O$ (S3)

$TeBr_4 + 2CsBr \rightarrow Cs_2TeBr_6$ (S4)

$TeO_2 + 4HI \rightarrow TeI_4 + 2H_2O$ (S5)

$TeI_4 + 2CsI \rightarrow Cs_2TeI_6$ (S6)

For reaction (1, 3, 5), stoichiometric amounts of TeO_2 and HCl/HBr/HI were stirred in a glass beaker. The precipitates were collected by filtration and washed several times with corresponding acid solution to remove unreacted materials. The powder was dried in an oven at 60 °C for 12 h.

Electrochemical measurements

2 M $ZnSO_4$ aqueous solution with 1 M acetic acid (HOAc) was used as a blank electrolyte. Subsequently, 0.3 M CsX (X=Cl, Br, I) was added to the blank electrolyte, resulting in the formation of CsCl, CsBr, and CsI electrolyte. The Swagelok cell was assembled with Zn plate anode (0.1 mm thickness, 12 mm in diameter), glass fiber separator (Whatman GF/A, 12.5 mm in diameter) and Te cathode (12 mm in diameter) with 10 or 100 μL electrolyte. The cells were galvanostatically charged/discharged on a NEWARE battery test system (Shenzhen, China) at 25 ℃. The electrochemical impedance spectroscopy (EIS) was performed on an INTERFACE1010 electrochemical workstation (Gamry, USA) using a 10 mV perturbation with a frequency range of 10 mHz to 1 MHz. Cyclic voltammetry measurements were performed on an electrochemical workstation (Gamry, USA). GITT (Galvanostatic Intermittent Titration Technique) tests has been performed to investigate the difference in diffusion kinetics between CsI and blank electrolytes. The diffusion coefficient was calculated based on Eq. S7:

$$D = \frac{4L^2}{\pi\tau}\left(\frac{\Delta Es}{\Delta Et}\right)^2 \quad \text{(S7)}$$

The duration of the current pulse (s) is represented by t, τ is the relaxation time (s), and ΔE_s means the steadystate potential change (V) by the current pulse. ΔE_t is the potential change (V) during the constant current pulse eliminating the iR drop. L is ion diffusion distance (cm), electrode thickness is often used to express its value.

Materials characterization.

Powder X-ray diffraction (XRD) was performed on D8 ADVANCE with Cu Kα radiation at a scan rate of 10 ℃ min^{-1} in 40 kV, 40 mA. Raman analyses were carried out on a bench Raman

dispersive micro spectrometer (InVia Reflex, Renishaw) using a laser (wavelength of 532 nm) at frequencies between 500 cm^{-1} and 100 cm^{-1}. UV–Vis spectrum characterization was carried out on a UV1902PC with a range from 190 to 600 nm. SEM studies were carried out on a Regulus 8100 field-emission SEM instrument. Electrodes were gently washed with deionized water to remove the electrolyte and dried for 6 h in vacuum oven at 40 °C before the characterizations. The zeta potential was measured using a Malvern Zetasizer NanoZS90.

Calculations

The Gibbs free energy was calculated using density functional theory (DFT) in DMol3 package. The structures were optimized at GGA-PBE functional with a DNP(4.4) basis set, including the dispersion correction (TS). The DFT semi-core pseudopot replaced the core electrons treatment. The implicit solvation model based on COSMO was applied during the structure optimization (Water/78.54). For the calculations of total energy, a global orbital cutoff of 5.0 Å was set, and the convergence tolerance of the energy, force, and displacement below 1.0×10^{-5} Ha, 2.0×10^{-3} Ha/Å, 5.0×10^{-3} Å were used for structural optimizations.

The adsorption energy (ΔE_{ad}) was defined as:

$$\Delta E_{ad1} = E_{Te+H_2O} - E_{Te} - E_{H_2O} \quad \text{(S8)}$$

$$\Delta E_{ad2} = E_{Te+Cs+I} - E_{Te} - E_{CsI} \quad \text{(S9)}$$

$$\Delta E_{ad3} = E_{Te+H_2O+Cs+I} - E_{Te+H_2O} - E_{CsI} \quad \text{(S10)}$$

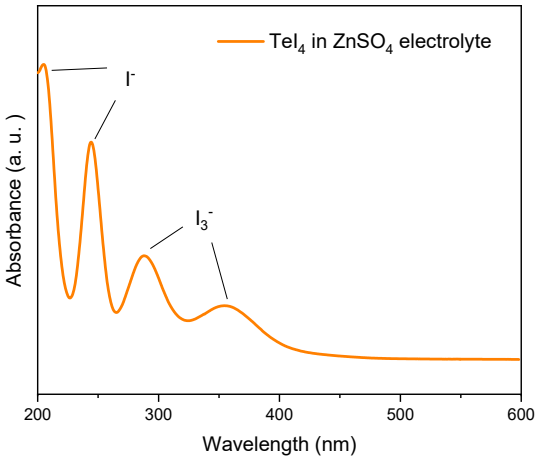

Figure S1 UV spectrum of the supernatant of TeI_4 powder in blank electrolyte.

The TeI_4 hydrolysis equation could be described as: $TeI_4+2H_2O \rightarrow TeO_2+4HI$. The oxygen in water further oxidize iodide ions to iodine: $O_2+2I^-+2H_2O \rightarrow 4OH^-+I_2$. Moreover, triiodide ions might be formed: $I_2+I^- \rightleftharpoons I_3^-$. The reaction might be accelerated under acidic conditions (the hydrolysis reaction produces HI). The UV spectrum of the solution confirms these reactions during the TeI_4 hydrolysis. These reactions lead to yellowish color of the TeI_4 hydrolysis solution.

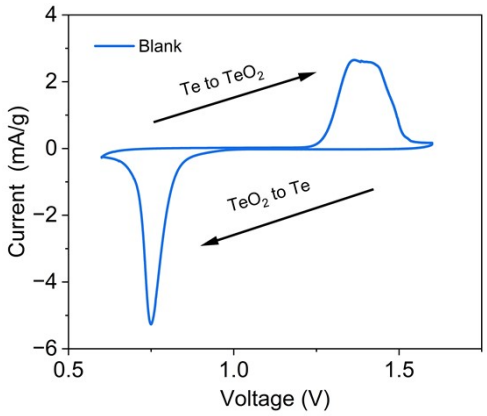

Figure S2. CV curve of Zn-Te battery in blank electrolyte at a sweep rate of 0.2 mV s^{-1}.

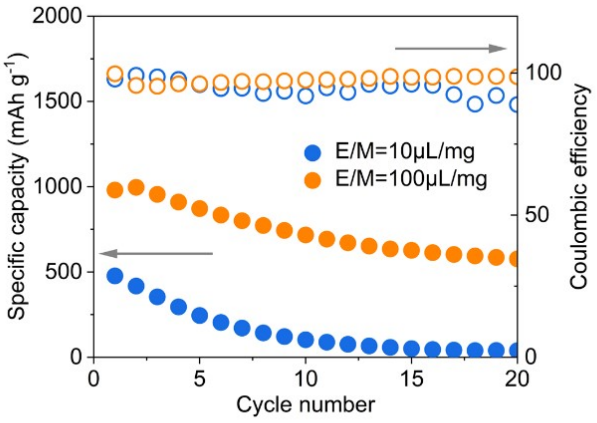

Figure S3. Cycling performance of Zn-Te cells in blank electrolyte with different electrolyte volumes.

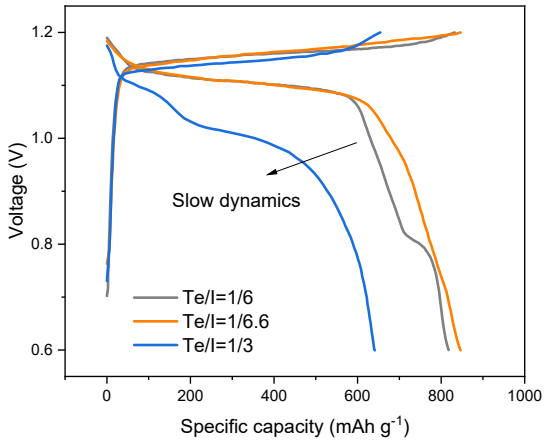

Figure S4. GCD curves of Zn-Te cells with different Te/I ratios.

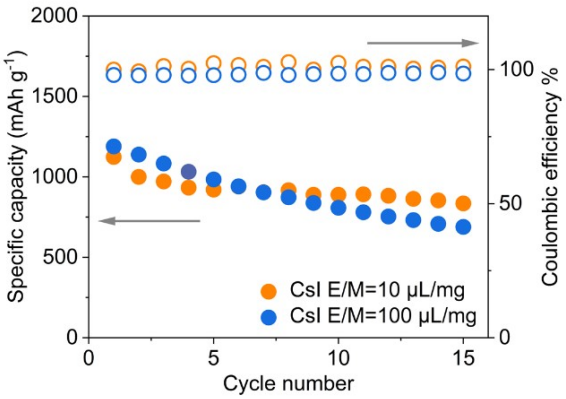

Figure S5. Cycling performance of Zn-Te cells in CsI electrolyte with different electrolyte volumes.

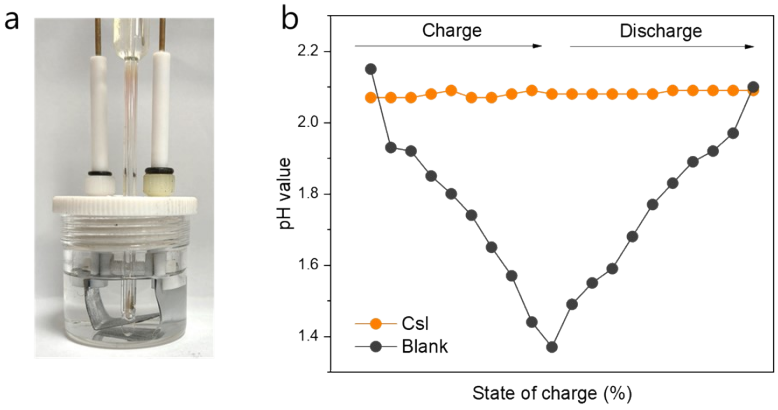

Figure S6 Variation of pH value during the charge/discharge process of 4e Zn-Te batteries in blank and CsI electrolyte.

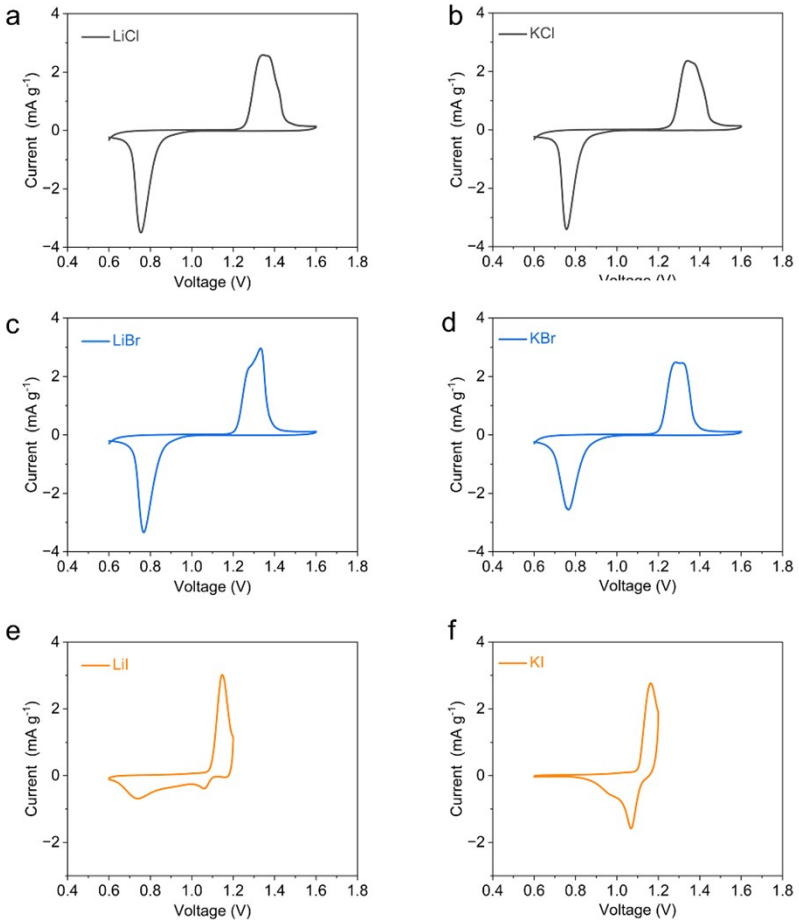

Figure S7. 4e CV curves of Zn-Te cells with different AX salts in the blank electrolyte.

Figure S8. Visualization experiments of the reaction between TeX_4 and AX salts.

Figure S9. The solid products obtained by adding different CsX in Figure S5 (a) CsCl; (b)CsBr; (c) CsI.

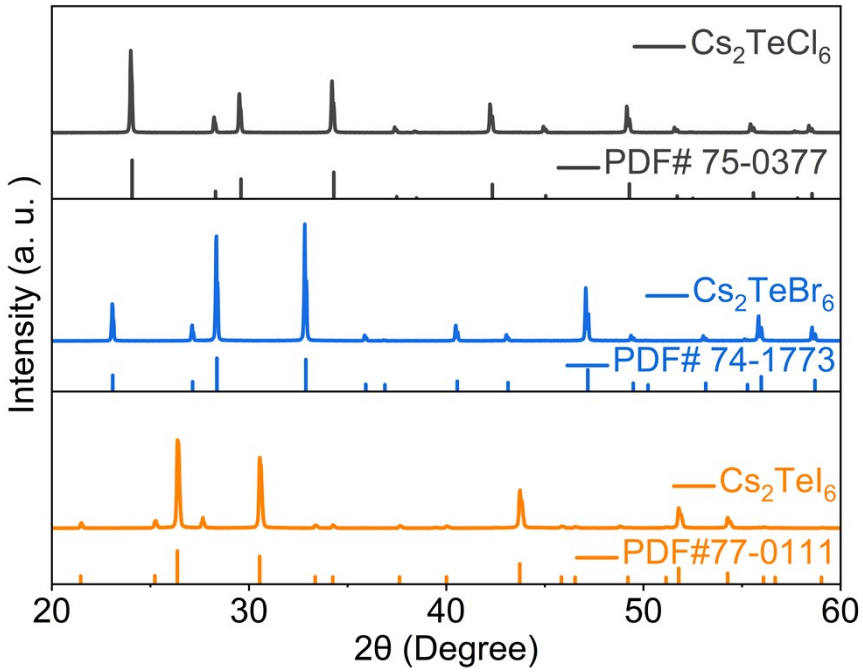

Figure S10. XRD pattern of Cs_2TeCl_6, Cs_2TeBr_6, Cs_2TeI_6

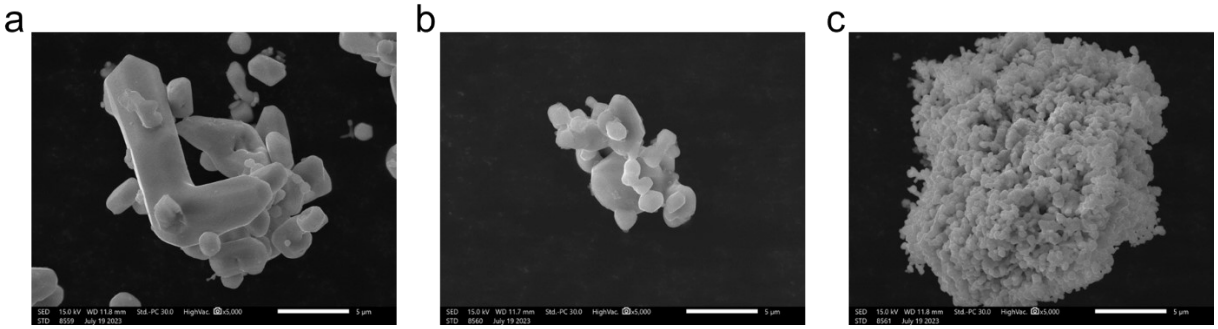

Figure S11. SEM images of Cs_2TeCl_6 (a), Cs_2TeBr_6 (b), Cs_2TeI_6 (c).

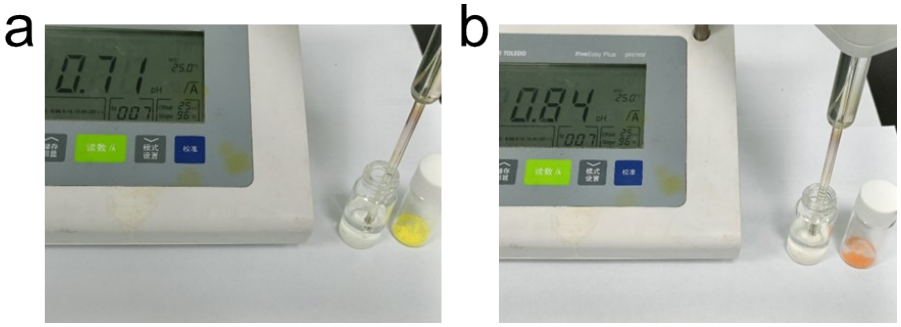

Figure S12. pH test after hydrolysis of a) Cs_2TeCl_6 and b) Cs_2TeBr_6.

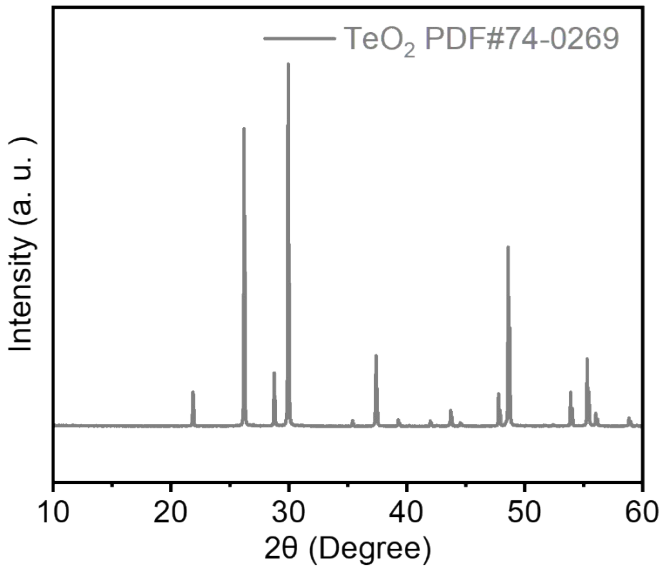

Figure S13. XRD characterization of the hydrolyzed precipitate obtained in Figure 3a (Cs_2TeCl_6 and (b) Cs_2TeBr_6).

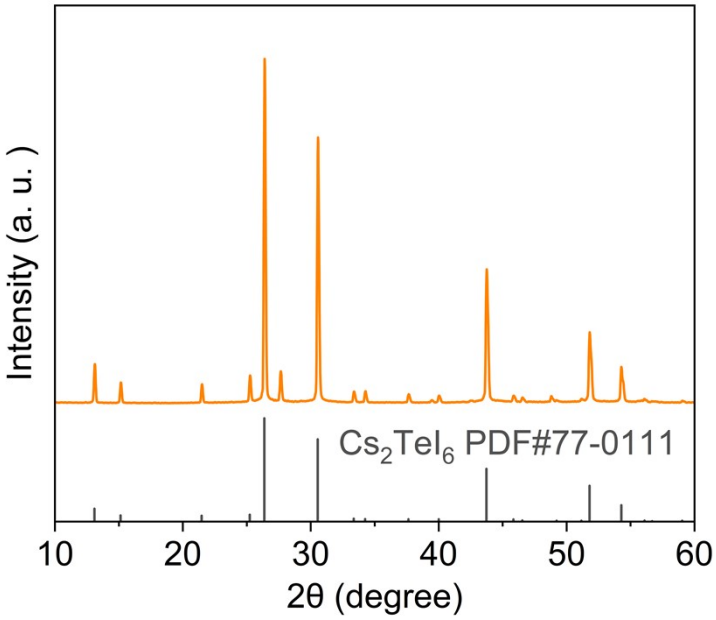

Figure S14. XRD pattern of the precipitate obtained in Figure 3a (Cs_2TeI_6).

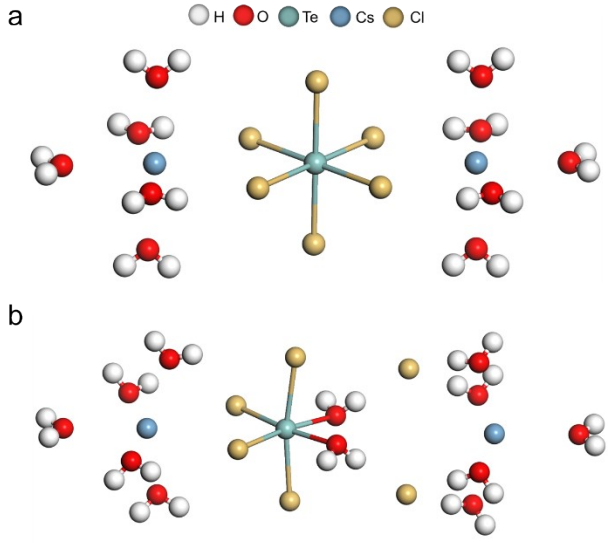

Figure S15. Hydrolysis model of Cs_2TeCl_6: a. Cs_2TeCl_6 with water molecule. b. $Te(H_2O)_2Cl_4$ with water molecule.

The corresponding hydrolysis reaction equation is as follows：

$$[Cs(H_2O)_5]_2\,TeX_6 + 2H_2O \rightarrow [Cs(H_2O)_5]_2\,[Te(H_2O)_2X_4]\,X_2 \qquad (S13)$$

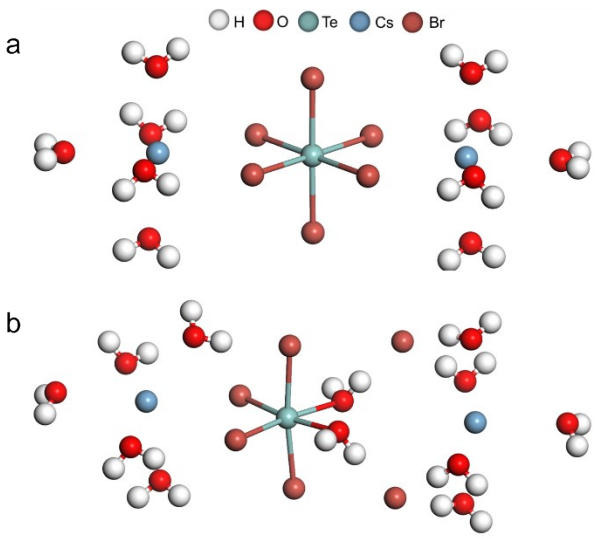

Figure S16. Hydrolysis model of Cs_2TeBr_6: a. Cs_2TeBr_6 with water molecule. b. $Te(H_2O)_2Br_4$ with water molecule.

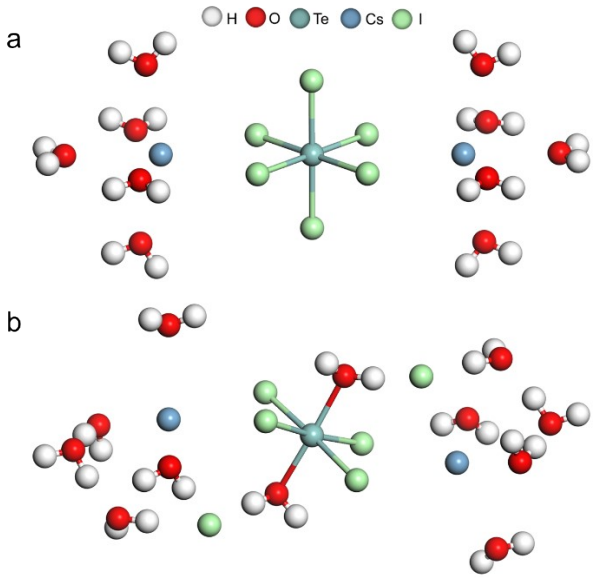

Figure S17. Hydrolysis model of Cs_2TeI_6: a) Cs_2TeI_6 with water molecule. b) $Te(H_2O)_2I_4$ with water molecule.

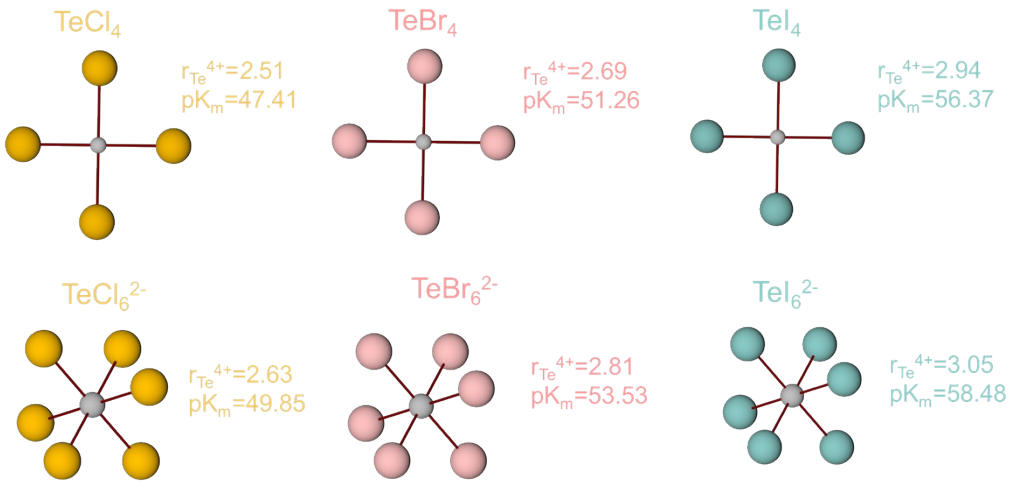

Figure S18. The hydrolysis constants pK_m of Te^{4+} cations in different coordinations.

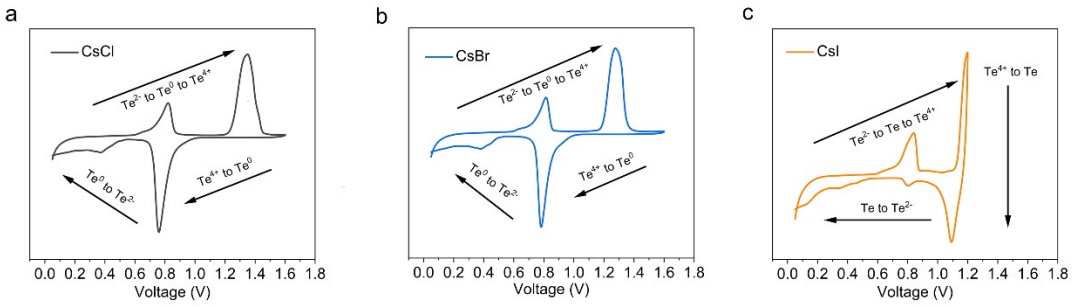

Figure S19. CV curves of the 6e process in different electrolytes at a sweep rate of 0.2 mV s^{-1}. a) CsCl. b) CsBr. c) CsI.

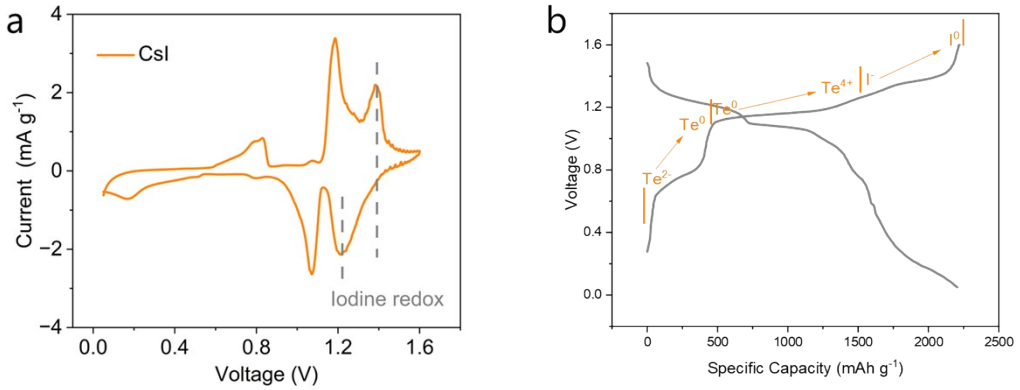

Figure S20. a) CV curve of the Zn-Te cell in the CsI electrolyte between 0.05-1.6 V. The sweep rate was 0.2 mV s^{-1}. b) GCD tests of the cell involves iodine redox.

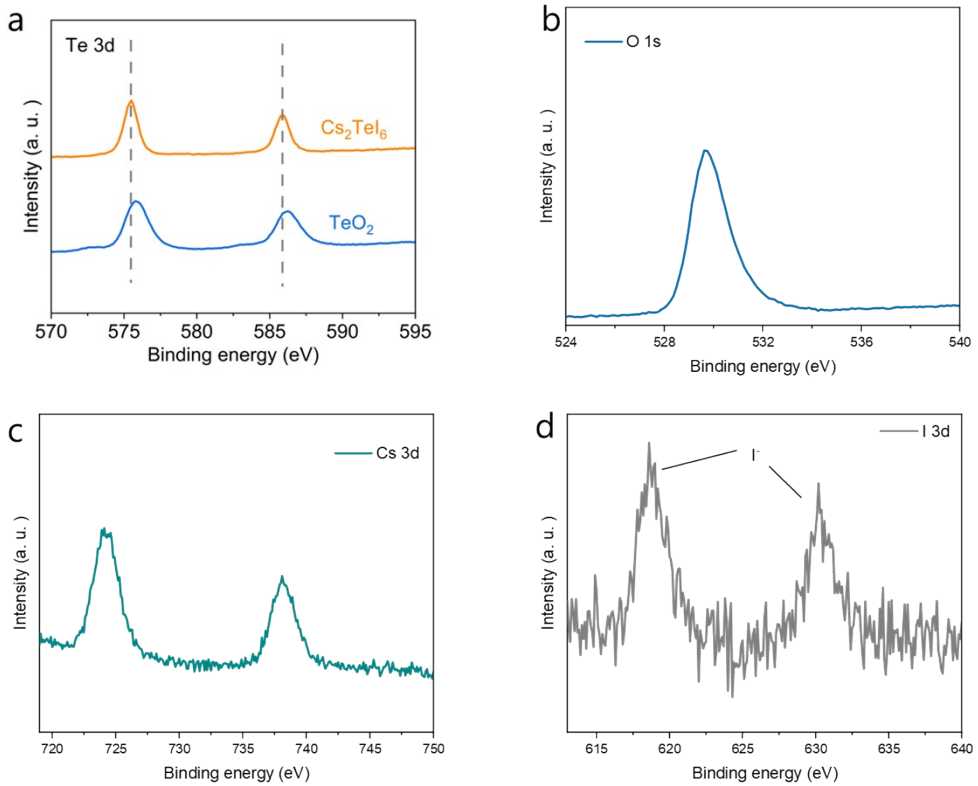

Figure S21. XPS spectrum of the Te electrodes after charged in CsI electrolyte (Cs_2TeI_6) and in blank electrolyte (TeO_2) in the charging state.

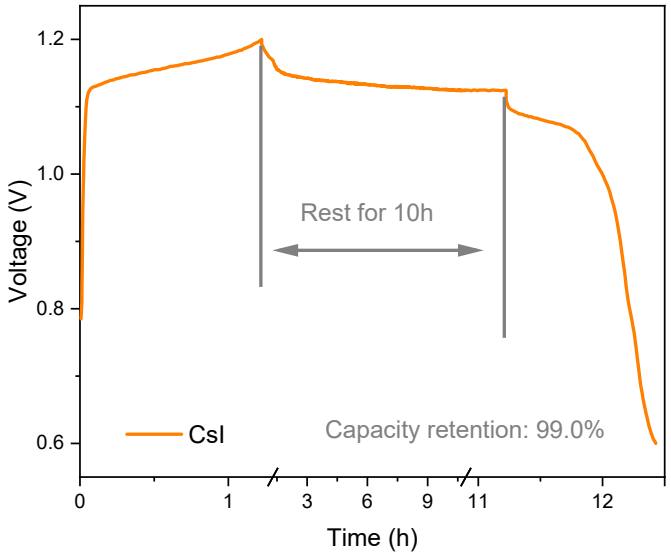

Figure S22. Self-discharge test of the fully charged Zn-Te cell in CsI electrolyte.

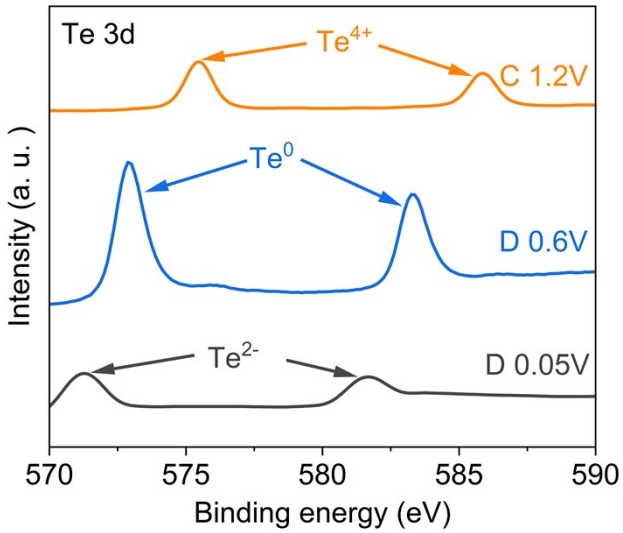

Figure S23. Ex-situ XPS spectrum of Te electrode at different states of charge in CsI electrolyte.

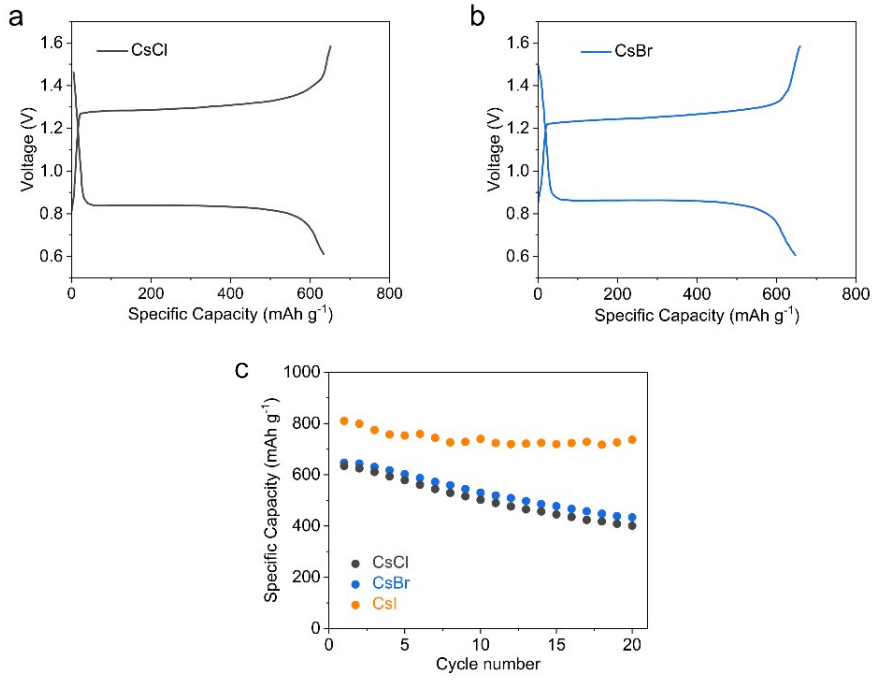

Figure S24. The electrochemical performance of Zn-Te cells in CsCl and CsBr electrolytes. a-b) GCD profiles. c) Cycle performance.

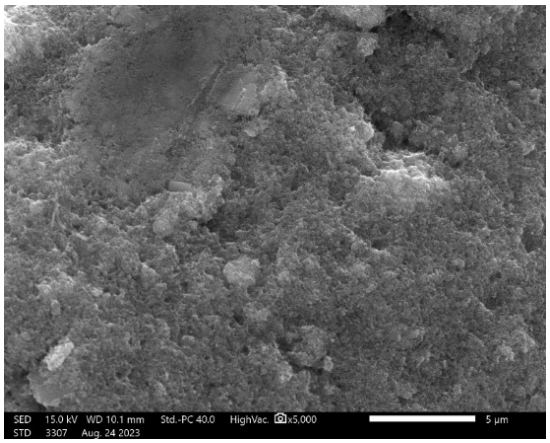

Figure S25. SEM image of the initail KB/Te electrode.

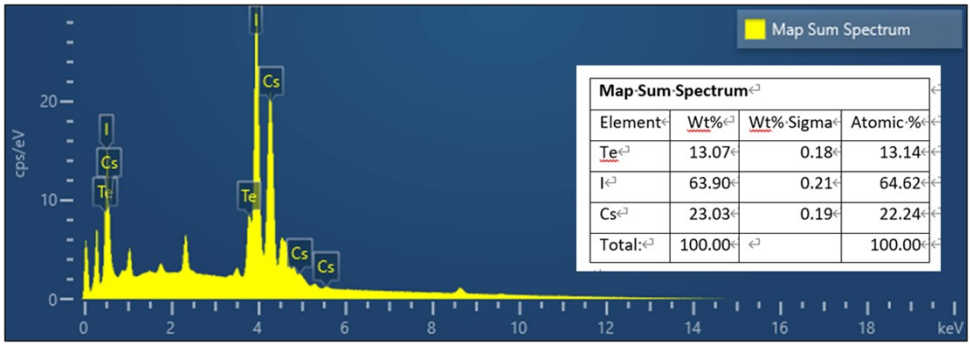

Figure S26. EDS profile of the fully charge Te electrode in CsI electrolyte.

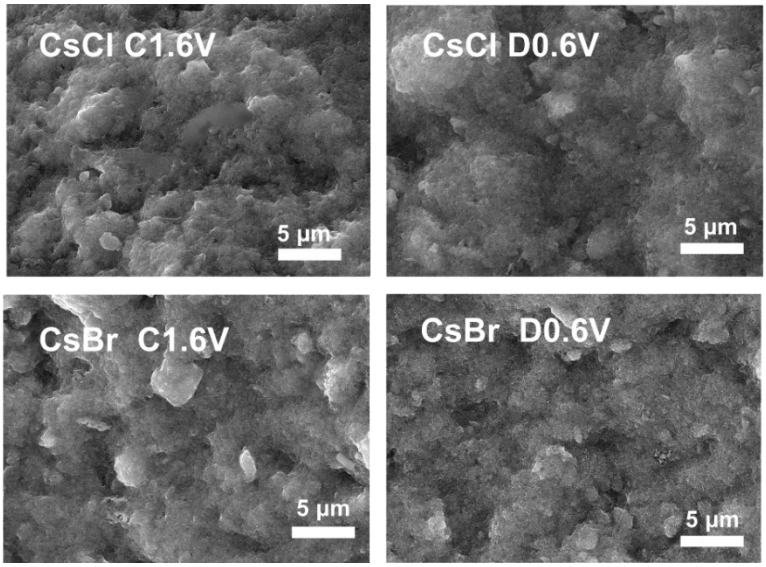

Figure S27. SEM images of the Te electrode at selected potentials in different electrolyte.

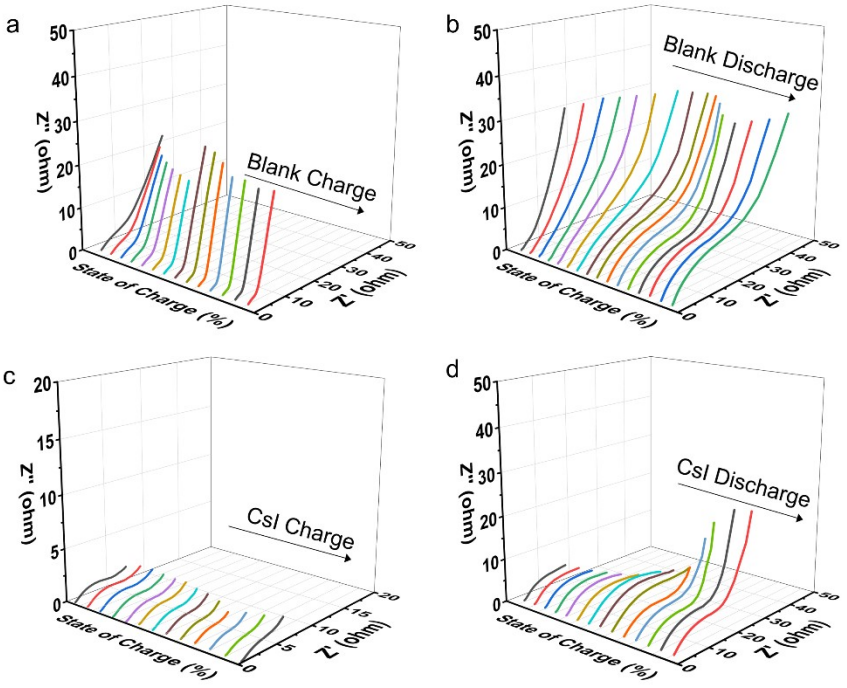

Figure S28. EIS profiles of Zn-Te cell at different state of charge. a, b) in blank electrolyte. c, d) in CsI electrolyte.

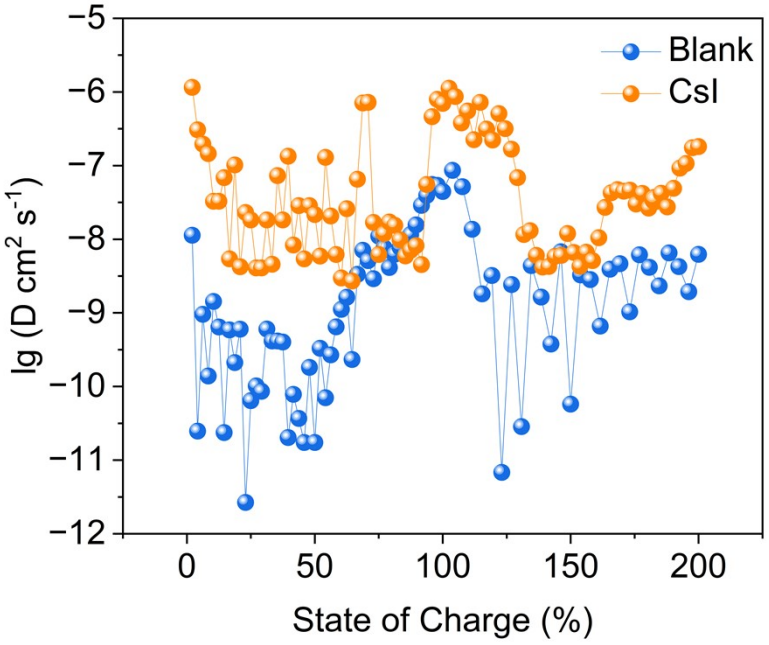

Figure S29. Diffusion coefficients of Zn-Te batteries during GITT measurement.

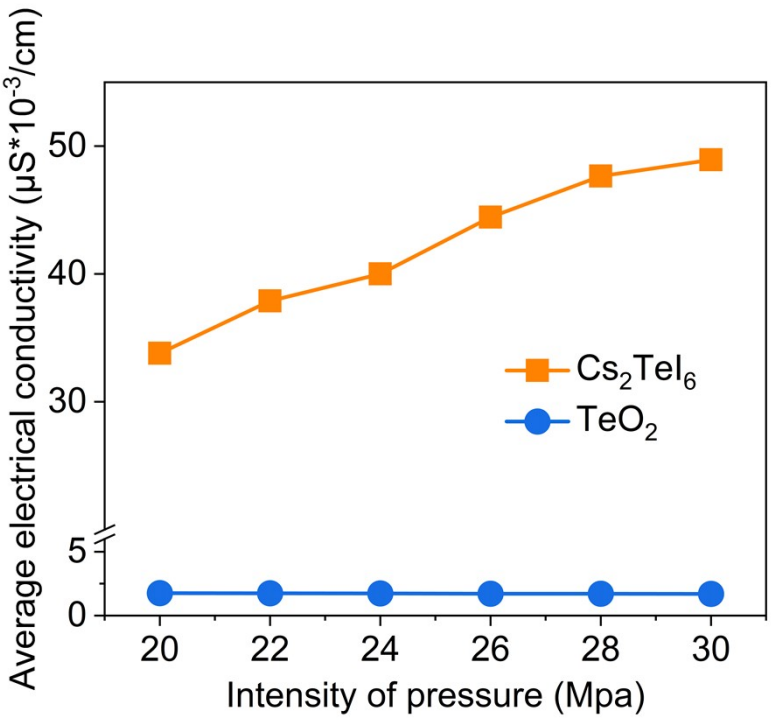

Figure S30. Electrical conductivity of the powdered materials.

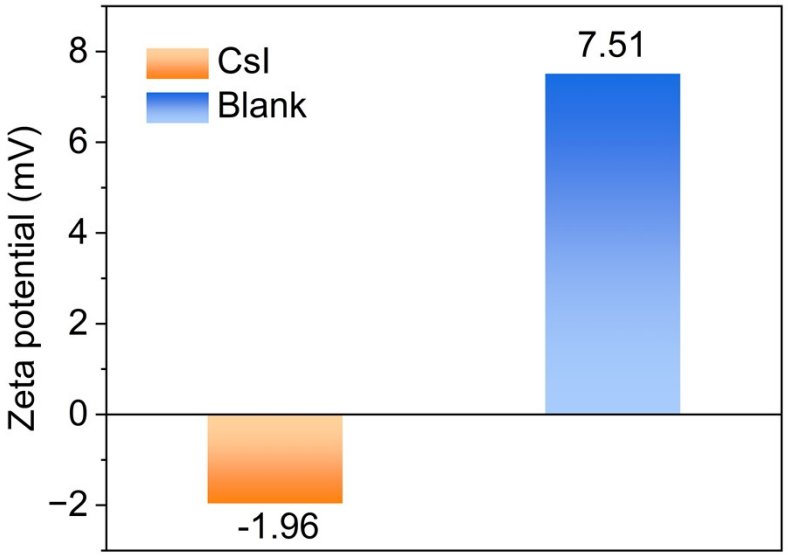

Figure S31. Zeta potential of KB/Te powder in different electrolytes.

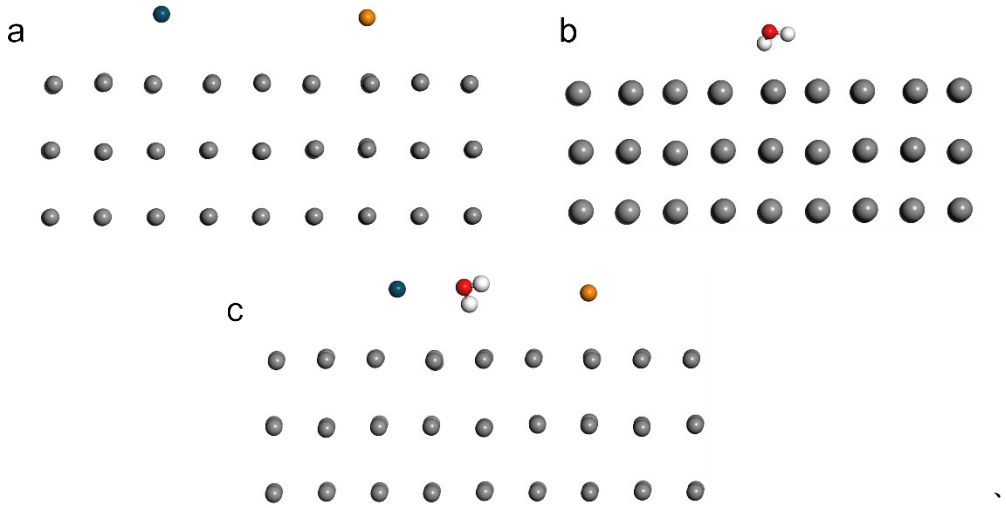

Figure S32. Different substances adsorbed on the surface of Te electrode a) CsI, b) H_2O and c) CsI + H_2O.

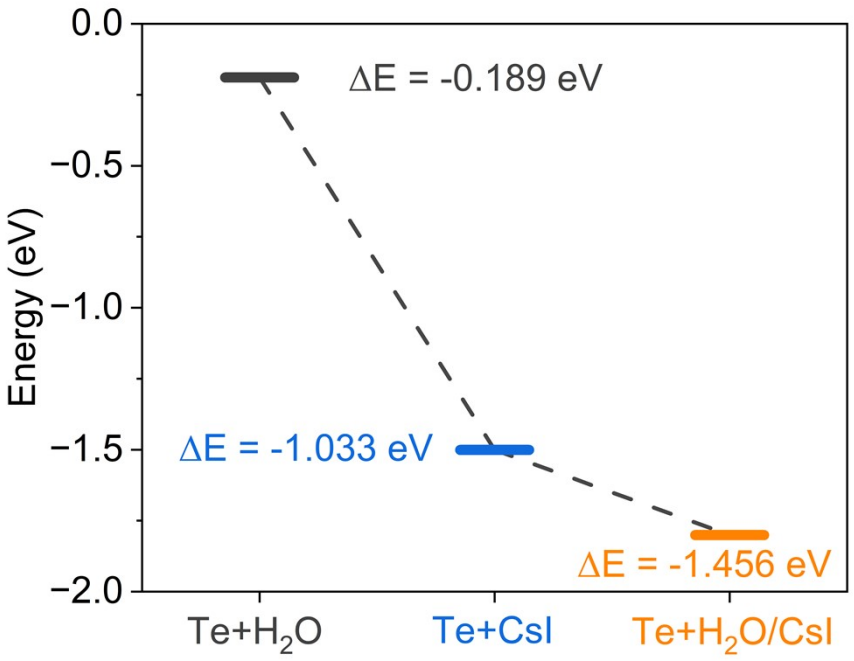

Figure S33. Comparison of adsorption energy on Te surface under different conditions.

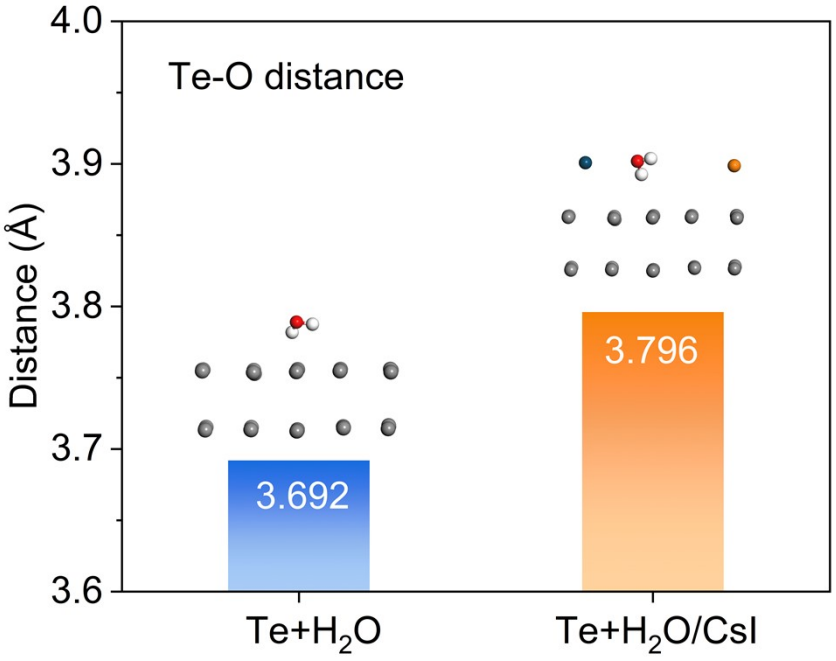

Figure S34. The distance between Te and O atom of absorbed H_2O obtained by DFT calculation.

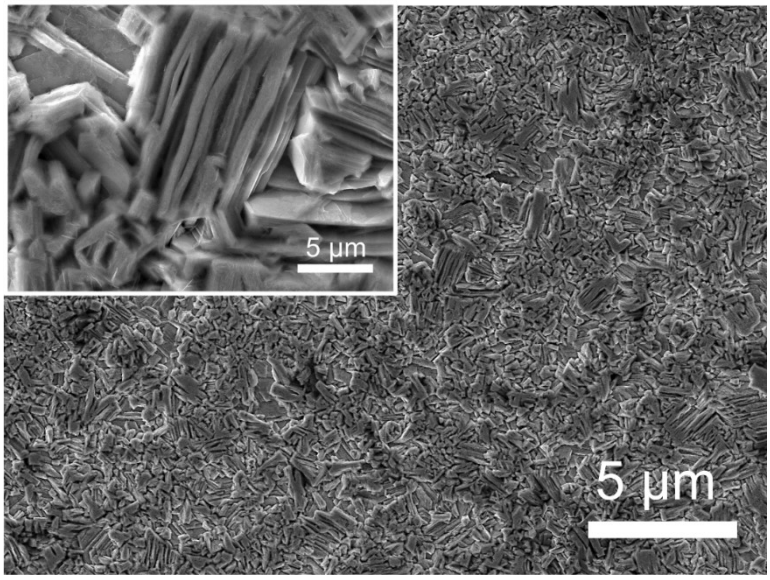

Figure S35. SEM images of the Zn cycled for 1 h at 1mA cm^{-2} in blank electrolyte.

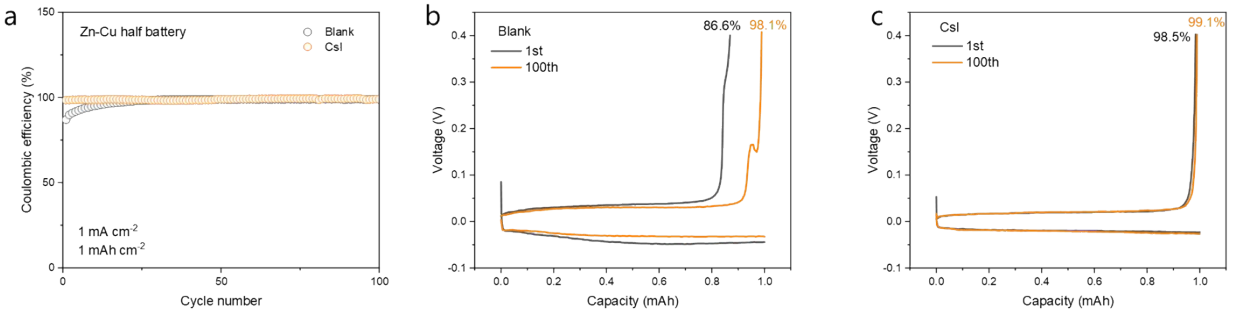

Figure S36 a) CE of Zn//Cu asymmetrical cells using blank and CsI electrolytes at 1 mA · cm^{-2}.
b-c) Voltage curves of Zn//Cu asymmetrical cells.

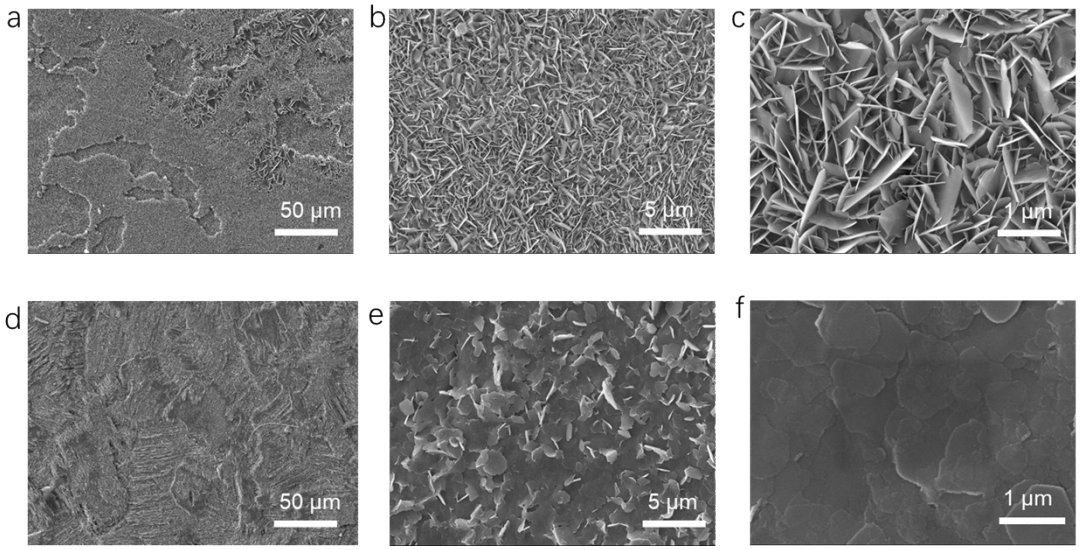

Figure S37. SEM images of Zn anode after plated with 10 mAh cm^{-2} in (a-c) blank，(d-f) CsI electrolyte.

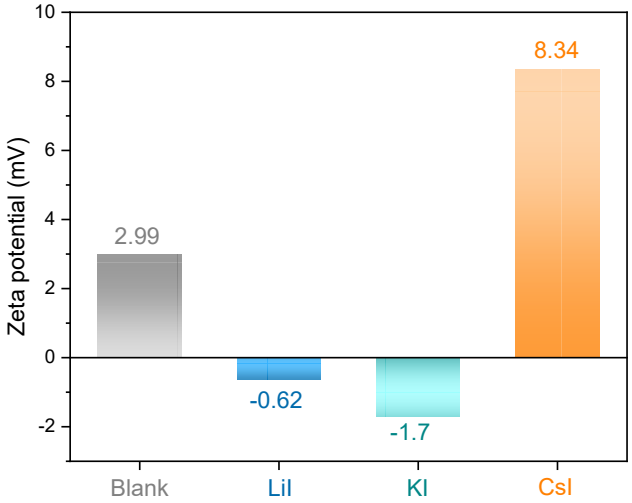

Figure S38. Zeta potentials of zinc anode in different electrolytes.

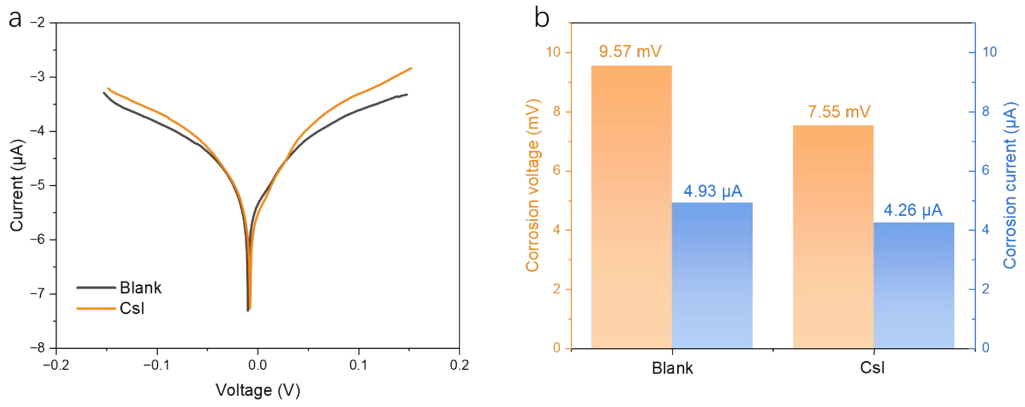

Figure S39. a) Linear polarization curves showing the corrosion of various electrolytes. b) The corrosion voltage and corrosion current of zinc anode various electrolytes.

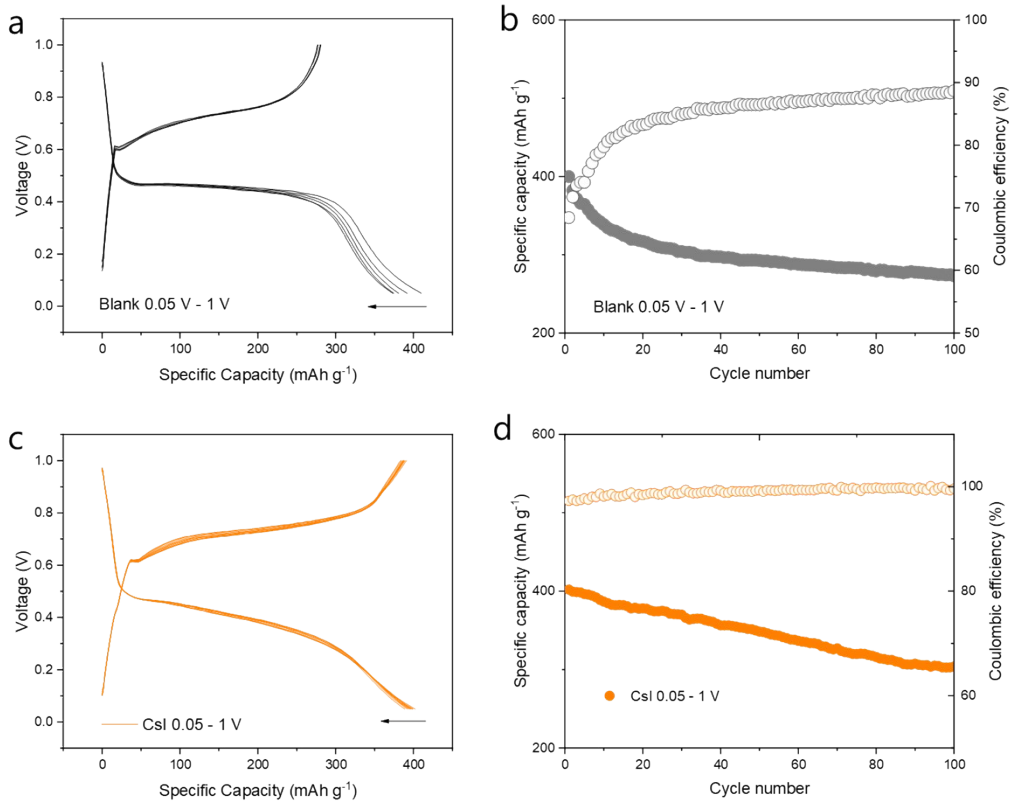

Figure S40. Electrochemical performance of 2e transfer process (Te ⇌ ZnTe) in Zn-Te cells with different electrolytes.

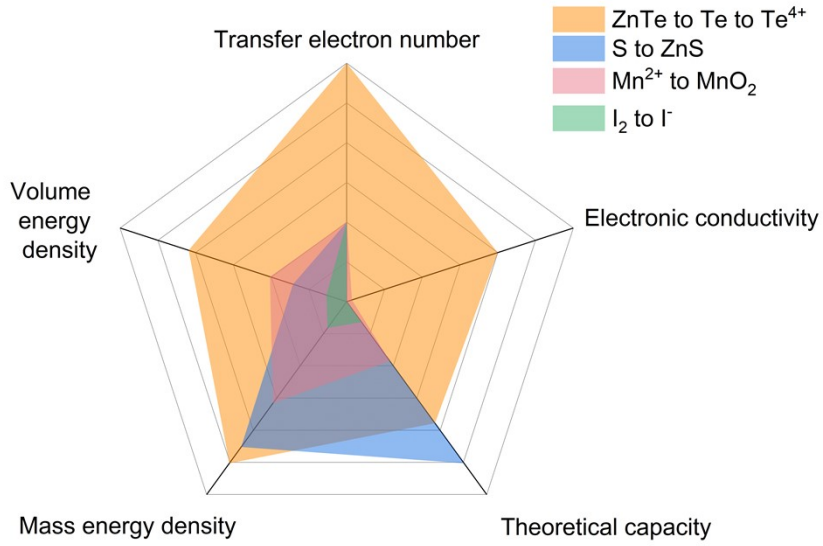

Figure S41. Performance comparison among different conversion reactions.

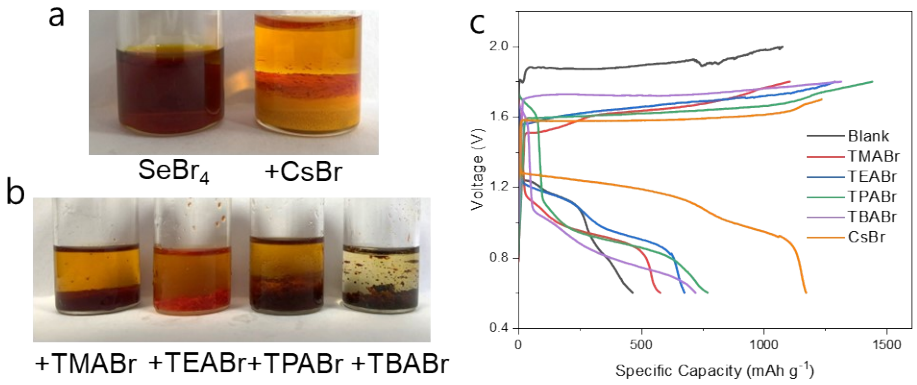

Figure S42. a-b) Visualization experiments of the reaction between SeX_4 and AX salts. c) Voltage profiles of Zn-Se cells with different electrolytes.

TMABr: Tetramethylammonium bromide, TEABr: Tetraethylammonium bromide, TPABr: Tetrapropylammonium bromide, TBABr: Tetrabutylammonium bromide.

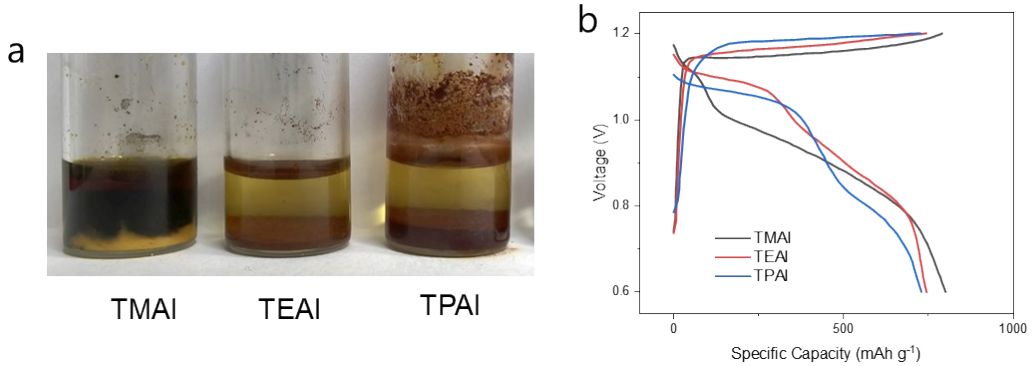

Figure S43. a-b) Visualization experiments of the reaction between TeX_4 and quaternary ammonium salts. c) Voltage profiles of Zn-Te cells with different electrolytes.

TMAI: Tetramethylammonium iodide, TEAI: Tetraethylammonium iodide, TPAI: Tetrapropylammonium iodide.